Toward Integrated Motion Planning and Control using Potential Fields and Torque-based Steering Actuation for Autonomous Driving

Enric Galceran, Ryan M. Eustice, and Edwin Olson

***Abstract*— This paper proposes an integrated motion planning and control approach for autonomous car navigation. Existing approaches to autonomous vehicle navigation typically plan a trajectory and pass it on to a steering controller that commands steering wheel angle (SWA) or curvature at every timestep to minimize tracking error. However, this approach exhibits large amounts of control effort, and ignores other criteria such as smoothness or the importance of staying on plan at different times. Conversely, our proposed approach leverages the concept of potential fields to represent a driving corridor with a desired tracking error tolerance and direct torque-based steering control to smoothly steer the vehicle with a much smaller control effort. Further, using potential fields allows us to naturally incorporate obstacles in the driving corridor to circumvent them, with typically no need for explicit trajectory planning. We compare our approach to a standard steering controller in experiments with a real-world autonomous vehicle platform. Results show that our proposed approach achieves similar path tracking performance as a high-gain SWA controller, but with much less actuator effort.**

I. INTRODUCTION

Most control systems in autonomous cars steer the vehicle using steering wheel angle (SWA) commands or, similarly, curvature commands (see, e.g., [1], [2], [3]). This approach has been shown to be moderately successful, especially throughout the DARPA Grand and Urban Challenges [4].

Nonetheless, using a position command (i.e. SWA or curvature) to steer the vehicle can be sub-optimal in some situations. Consider for instance a vehicle making a 90-degree turn at an intersection. Throughout the turning maneuver, external forces will act on the steering column, most conspicuously self-aligning torque, which tends to align the tires along the vehicle's direction of travel. A position-based controller will "fight" those forces during the entire maneuver, exerting a large amount of control effort to keep the steering wheel at a sequence of exact angles to track the cornering path. This vividly contrasts with how a human driver would intuitively exploit the restoring forces once the vehicle is heading toward the end of the turn, that is, relaxing the torque applied to the steering wheel and allowing the restoring forces to align the vehicle along the path rather than forcing the steering wheel at particular angles.

Similarly, when driving along a lane with only mild curves at close to constant speed (which encompasses a great part of all driving situations), there appears to be no need to force the steering wheel at a particular angle: human drivers typically apply a very subtle torque to the wheel to roughly center the car in the lane. Small cross track errors in an uncrowded lane are accepted by human drivers. Conversely, tracking a precise path along the center of the lane via steering position commands is likely to achieve small cross-track error, but at the cost of a large, unnatural effort applied to the wheel.

Further, a position-based steering controller ultimately needs to command the torque applied to the steering system that will make the wheels turn. This requires a non-linear mapping from position to torque, likely involving additional control loops and look-up of boost curves (static maps to provide the correct amplification to the driver's exerted torque) that increase latency and introduce many model parameters that can be hard to determine.

In this work, we argue that, while this scheme of precision

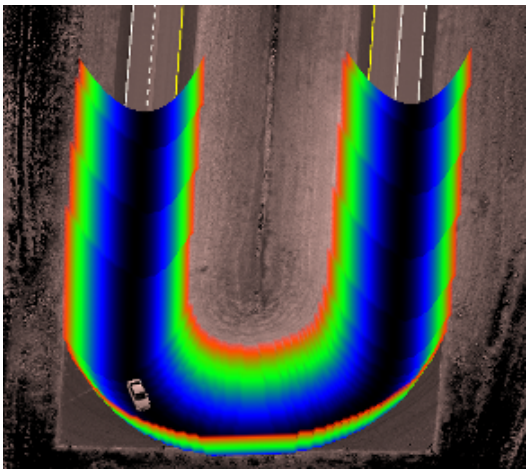

Fig. 1: Visualization of the proposed integrated motion planning and control approach controlling an autonomous vehicle negotiating a hairpin curve. The car avatar marks the vehicle's pose, and the potential field used to compute the steering torque commands sent to the vehicle is represented as a height-colored elevation map. The potential field approach naturally defines a nominal driving corridor, allowing to smoothly steer the vehicle directly commanding torque applied to the steering column. A metric-topological representation of the road network (solid and dashed lines) and a LIDAR intensity map (grayscale) are shown for reference and scale.

This work was supported in part by a grant from Ford Motor Company via the Ford-UM Alliance under award N015392 and in part by DARPA under award D13AP00059.

The authors are with the University of Michigan, Ann Arbor, MI 48109, USA. {egalcera,eustice,ebolson}@umich.edu

steering might be useful for tracking "threading-the-needle" paths, as may be required in parking maneuvers or sharp turns, there are many situations in which steering the vehicle using a direct torque input has the potential to yield more natural driving behavior and lower control effort.

To this aim, we present an integrated motion planning and control approach that leverages a torque-based steering interface in conjunction with potential fields [5] to command an autonomous vehicle. Using potential fields allows to define a driving corridor with some acceptable tolerance (e.g., driving along a lane), as opposed to following an arbitrarily stringent trajectory (e.g., tracking the center of a lane). In this way, planning and control are unified, since the controller is aware of how serious tracking errors are (or are not), being able to adapt its response accordingly. In contrast, traditional approaches typically employ a fixed and high gain regardless. Furthermore, potential fields provide a connection between planning and control by being able to readily incorporate obstacles in the environment, yielding steering commands that can smoothly circumvent them. The visualization in Fig. 1 illustrates the proposed approach.

Our approach seeks to

1) leverage a direct steering torque input to more naturally exploit external forces on the vehicle to counter steer,
2) use a potential field to reflect the importance of remaining on a specific path at each point in space and time and to easily account for obstacles,
3) require less dependence on precise models of the system (e.g., mappings from SWA to steering torque), which are complex given the external forces on the car and subject to change from vehicle to vehicle.

We show the feasibility of the proposed approach in a series of runs with an autonomous vehicle on a closed test track, demonstrating free-form steering maneuvers, following of tightly curved roads and obstacle avoidance capabilities. Further, we compare our approach to a SWA-based steering controller in terms of path tracking error and control effort. Our results show that our approach achieves a similar level of path-tracking error at a significantly lower control effort.

We note that, in this work, we focus on steering or lateral control of the vehicle, whereas longitudinal or speed control is assumed to be handled by an appropriate control module, as is the case for the autonomous vehicle platform we use in our experiments.

II. RELATED WORK

Most autonomous car platforms developed up to date approach the navigation problem (that is, safely driving the vehicle to a desired goal) by first planning a specific path to a goal and then tracking it using a feedback controller. Such nominal path is typically obtained using search-based planning algorithms [6], sampling-based planning [7] or numerical optimization [8]. Once a path is available, it is typically tracked by the controller using SWA or curvature commands with the primary objective of minimizing tracking error (see, e.g., [1], [2], [3]), leading to the aforementioned disadvantages. Further, large amounts of computational resources are spent on finding a collision-free path in the planning phase.

The concept of a driving corridor is common in mobile robotics, although they are often conceived to represent obstacle-free regions of the environment, such as in the work of Geraerts and Overmars [9] and Wein et al. [10]. More similarly to our approach, Dolgov et al. [11] develop a local-minima-free cost-map based on a Voronoi decomposition of the robot's static obstacle map. However, the driving corridor we propose in this work is defined in terms of a potential field designed to provide an easily differentiable potential function that is convex with respect to the lateral offset of the vehicle from the center of the nominal path, and is directly related to the torque input applied to steer the vehicle.

Potential fields for robotic navigation are certainly not new, originating almost three decades ago (see [5] for a tutorial). Wolf et al. proposed artificial potential functions for highway driving [12], but their results are limited to simulations. However, in this work we adopt the concept in combination with a torque-based steering controller for smooth steering of an autonomous vehicle, circumventing the limitations of potential fields when applied to non-holonomic systems and arbitrarily complex obstacle maps [13]. Other researchers have proposed controlling steering torque directly [14], [15], although these approaches focus on trajectory tracking rather than exploiting perceptual information of the vehicle's surroundings such as the presence of other traffic participants or the deviation from the lane center.

III. METHOD

Our proposed integrated motion planning and control method consists of two main components: a driving corridor constructed using a potential field and a steering controller that exploits a torque-based steering interface. The potential field is composed of a steering component that guides the vehicle toward its nominal path and obstacle potentials driven by the presence of static obstacles and other vehicles participating in traffic.

A. Potential Field

We construct a potential field to represent the vehicle's driving corridor by means of a potential energy function $U : \mathbb{R}^2 \to \mathbb{R}$:

$$U(x) = U_{\text{att}} + U_{\text{rep}}, \tag{1}$$

where x is a point on the vehicle's 2-dimensional plane, U_{att} is the *attractive* potential that guides the vehicle toward the nominal path and U_{rep} is the *repulsive* potential that vectors the vehicle away from obstacles in the environment. The objective of the vehicle is to minimize the energy of this potential by commanding a steering torque input based on the negative gradient of the potential energy function:

$$-\nabla U(x) = -DU(x) = -\left[\frac{\partial U}{\partial x_1}(x), \frac{\partial U}{\partial x_2}(x)\right]^\top. \tag{2}$$

We generate the attractive potential U_{att} around a nominal path of travel (e.g., the lane center), which can be obtained,

for instance, from a prior road network map or using a motion planner (see, e.g., [16], [17]). Given a nominal path Π as a sequence of N 2-dimensional waypoints $\Pi = w_1, \ldots, w_N$, we consider attractive potentials $U_{\text{att}}(x)$ for all points x in a local neighborhood of the vehicle of the form

$$U_{\text{att}}(x) = d^i(x, \Pi),\ i \in \mathbb{N},\ i > 0, \tag{3}$$

where $d(x, \Pi)$ is the distance from a point x to its closest segment in the path Π. We have empirically found a quadratic potential, i.e., $i = 2$ to provide sufficient control authority to steer the vehicle on the nominal path, whereas a linear potential ($i = 1$) required a high proportional gain on the feedback controller (see Section III-B below) leading to instability, and higher orders ($i > 2$) did not provide substantially different performance compared to a quadratic potential. Thus, we define our potential as

$$U_{\text{att}}(x) = d^2(x, \Pi). \tag{4}$$

The quadratic cost function in Eq. 4 avoids local minima by having a zero cost centerline, is convex with respect to the robot's lateral offset in its nominal path, and allows for straightforward calculation of derivatives even within obstacle regions.

Fig. 1 shows an example of an attractive potential field generated at a hairpin curve section of a test track, following the center of a desired lane of travel.

Similarly, we use a quadratic potential U_{rep} in the vicinity of obstacles (we discuss a test run of our system involving a repulsive potential below in Section V-C). By adding the attractive and repulsive potentials, we obtain the total potential $U(x) = U_{\text{att}} + U_{\text{rep}}$ whose potential function, per Eq. 2, is given by

$$F(x) = -\left|\left|\nabla U(x)\right|\right|. \tag{5}$$

While local minima in potential fields are a problem for systems that use them to make progress toward a goal location [13], here the potential field is specifically constructed to control the vehicle's steering actuator (leaving out longitudinal control), and therefore any minimum therein represents an acceptable corridor for the vehicle to drive through. The degenerate case where the driving corridor is completely blocked by obstacles is easily handled by the longitudinal control module, commanding the vehicle to stop upon that circumstance.

A shortcoming of most potential field methods is that they complicate analysis of the closed-loop control system. However, since our potential $U(x)$ is a quadratic function, its gradient is given as

$$\nabla U(x) = \left[\frac{\partial U}{\partial x_1}(x), \frac{\partial U}{\partial x_2}(x)\right]^\top = [C_1 x_1, C_2 x_2]^\top, \tag{6}$$

where C_1 and C_2 are constants. Therefore, $F(x)$ is equivalent to a proportional gain obtained from the potential field. However, a proportional gain does not suffice to stabilize the system at hand, which if approximated by the simplified system $\ddot{\Psi} = \tau$ (where $\ddot{\Psi}$ is the yaw acceleration of the vehicle and τ is the applied torque) is at least second-order. This theoretical limitation is further supported by initial tests with our autonomous vehicle system. Thus, we put forward the following feedback steering controller.

B. Torque-based Steering Controller

Given the potential field introduced above, we use a proportional-derivative (PD) feedback controller to issue a torque command to the steering system as a function of the potential field. The control objective is to steer the vehicle following the potential function in Eq. 5, as shown in Fig. 1.

More precisely, the input variable to the controller is the potential function $F(x_{t+L})$, evaluated at a point x_{t+L} located at some lookahead time L seconds in the future, where x_t is the position of the center of the rear axle of the vehicle at time t. Thus, the torque command at time t is given as

$$\tau(t) = K_p F(x_{t+L}) + K_d \frac{d}{dt} F(x_{t+L}), \tag{7}$$

where K_p is the proportional gain and K_d is the derivative gain (tuning parameters). The block diagram of the feedback controller is shown in Fig. 2.

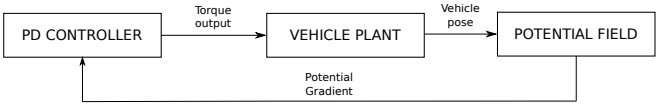

Fig. 2: PD feedback control loop for torque-based steering.

IV. EXPERIMENTAL SETUP

A. Test Surfaces

We have evaluated our proposed approach using our autonomous vehicle platform on several runs on different surfaces of a test track located at the Dearborn Development Center (DDC) facilities of the Ford Motor Co., using the vehicle dynamics area (VDA), steering and handling course (SHC) and low speed straightaway (LSSA) test surfaces (Fig. 3). The VDA test surface provides an ample paved space to perform free-form steering runs, the SHC consists of a narrow two-lane road with sharp curves and pronounced slope changes, and the LSSA consists in a two-lane loop with two long straightaways.

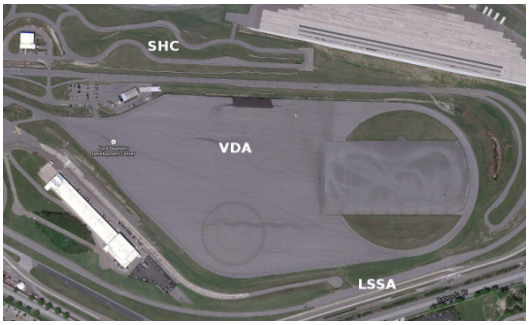

Fig. 3: Test surfaces at Ford's DDC used in our experiments. Image credit: Google, Digital Globe, Sanborn, U.S. Geological Survey, USDA Farm Service Agency.

B. Experimental Platform

The experimental platform we use in our experiments consists of a Ford Fusion vehicle, equipped with a drive-by-wire system featuring a steering interface that can be configured to accept either SWA or torque requests.

The vehicle, shown in Fig. 4, is equipped with four Velodyne HDL-32E 3D LIDAR scanners, an Applanix POS-LV 420 inertial navigation system (INS), GPS, and several other sensors. An onboard five-node computer cluster performs all planning, control, and perception for the system in realtime. In particular, our implementation of the proposed approach runs onboard the vehicle at 20 Hz.

Fig. 4: Our autonomous car platform, a Ford Fusion equipped with four LIDAR units, survey-grade INS, and a steering interface able to operate in both SWA and steering torque mode. All perception and control is performed onboard.

The vehicle uses prior maps of the area it operates on, which capture information about the environment such as LIDAR reflectivity and road height, and are used for localization, obstacle detection, and other perceptual tasks. The road network is encoded as a metric-topological map using a derivative of the route network definition file (RNDF) format [4], providing information about the location and connectivity of road segments and lanes therein. Desired paths of travel can be obtained leveraging this prior knowledge.

Estimates over the states of other traffic participants are provided by a dynamic object tracker running on the vehicle, which uses LIDAR range measurements. The geometry and location of static obstacles are also inferred on board using LIDAR measurements.

V. RESULTS

We now present preliminary results obtained after evaluating the proposed approach on our autonomous vehicle platform. We initially run straight line maneuvers and free-form steering maneuvers with increasing curvature on the VDA surface, moving at low forward speeds ($\sim$4 m/s). We then evaluated the performance of the system on several runs on the SHC, moving at speeds up to 7 m/s. Finally we performed several runs with maneuvers involving the presence of obstacles (i.e., involving potential fields with obstacle components) again on the VDA at lower speeds. We use a lookahead time $L = 1.5$ s in all experiments.

A. Initial Tests

As a first validation of our proposed approach, we run several free-form steering trials on the VDA surface and following of straight line paths on the LSSA. We were able to successfully steer the vehicle along a nominal path using an associated potential field such as that shown in Fig. 5. The nominal paths included several different curvatures, and all were tracked at a constant longitudinal speed of 4 m/s.

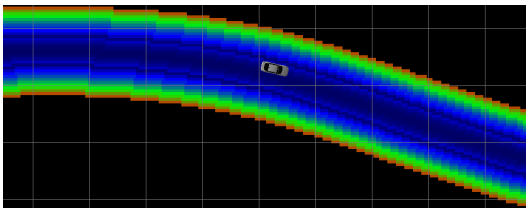

Fig. 5: Our vehicle navigating through one of the potential fields generated on the VDA surface (top view). Notice that the vehicle incurs a slight lateral offset from the potential field's zero-level curve. However, it is a perfectly acceptable zone of the potential field for the vehicle to navigate on, allowing it to tackle the curve following a relaxed trajectory, with no need to stringently track the center of the nominal path as a standard SWA-based steering controller would do.

B. Steering and Handling Course

On the SHC we are able to test our approach and compare it to a SWA-based steering controller, following the same nominal path along the course, being approximately 1.5 km long. The SWA-based controller uses a kinematic model of the car to command a SWA value to track the nominal path minimizing cross-track error, operating in a way similar to the pure pursuit path tracking algorithm [18]. We first show the performance of both approaches in terms of torque applied to the steering system, and then we compare both approaches in terms of path tracking error and control effort.

Fig. 6 shows the performance of our proposed approach in terms of the input signal to the controller, $\nabla F_t(x_{t+L})$, and the output (torque applied to the steering system). The steering torque applied by the SWA-based controller is shown in Fig. 7. It can be observed that our proposed approach produces some low frequency oscillations in the torque signal, but the steering behavior from a rider's perspective does not differ qualitatively from that typical of a human driver. Conversely, as a result of rigidly seeking to lock the wheel at a particular angle, the SWA-based controller exerts a very high-frequency torque on the steering system.

We now quantitatively compare the performance of our proposed approach and the SWA-based controller in terms of path tracking error and control effort. The path tracking error is computed as the signed distance between the vehicle's position and the closest segment in the path, being positive if the car lays to the right of the path and negative otherwise, while the control effort is given as the amount of work done

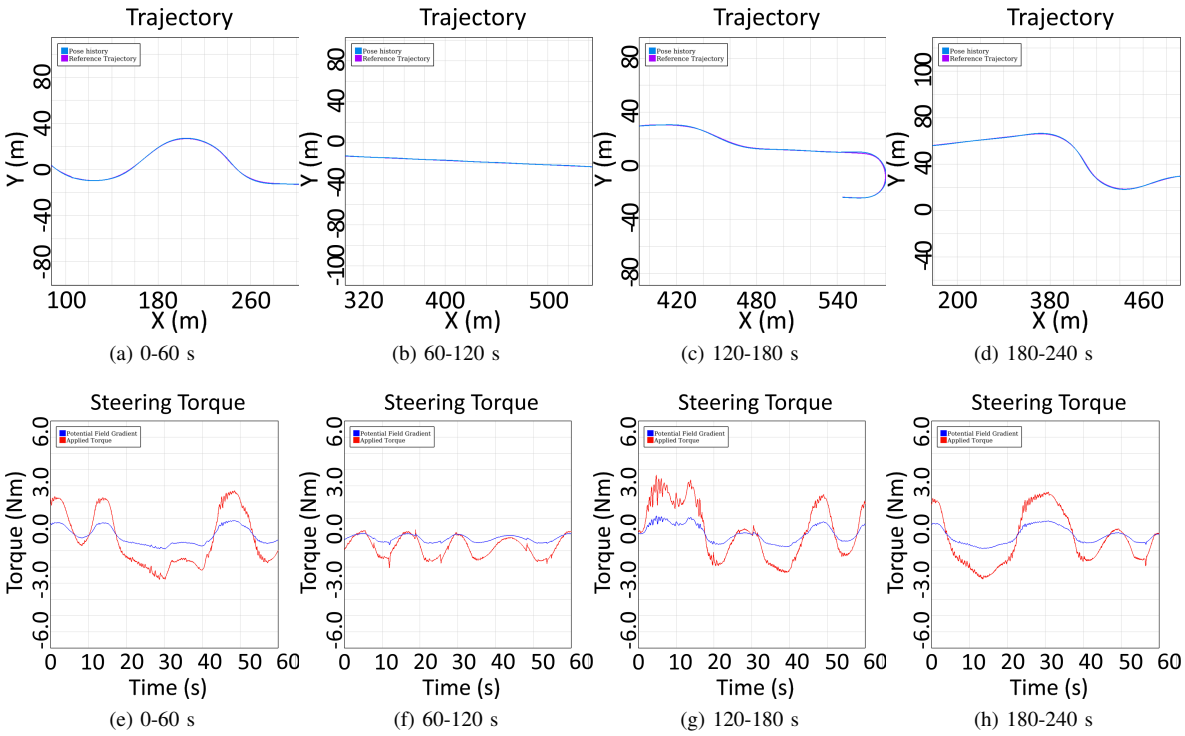

(a) 0-60 s (b) 60-120 s (c) 120-180 s (d) 180-240 s

(e) 0-60 s (f) 60-120 s (g) 120-180 s (h) 180-240 s

Fig. 6: Sections of the vehicle's executed trajectory (top row) and controller input and output (bottom row) on a trial on the SHC using our proposed approach.

by the actuator:

$$W = \int_{t_0}^{t_f} |\tau(t)|\, d\theta \quad [\text{J}], \tag{8}$$

where $\tau(t)$ is the torque applied to the vehicle's steering system at time t, t_0 and t_f are the start and end instants of the run, respectively, and θ is the steering column angle.

Fig. 8 shows the path tracking error along a typical test run for our proposed approach and the SWA-based controller, while Fig. 9 shows the control effort. Notice that, due to differing longitudinal speeds, the trajectories have different durations: the trajectory traced by our proposed approach lasts 255 s and the trajectory traced by the SWA-based controller lasts 160 s. We are working to run experiments under similar longitudinal speeds. However, the nominal path is the same for both controllers and hence it places the same challenge to both approaches in terms of steering.

Both controllers offer similar path tracking performance, operating within 30 cm accuracy for most of the trajectory. Our proposed controller presents a noticeable peak at just under 90 cm tracking error at half way through the trajectory, when passing through the tight hairpin curve. This occurs because a very large steering effort is required in that area, and our approach, not including a precise kinematic model of the system, trades off tracking precision for smoother steering behavior. However, the SWA-based controller presents high peaks well above 60 cm error likewise.

In terms of torque effort, however, our proposed approach accumulates approximately 1500 J during the run, while the SWA-based controller requires more than 4500 J of work. This significant difference evidences the smoother steering behavior exhibited by our proposed approach.

C. Incorporating Obstacles on the Potential Field

An interesting feature of the proposed integrated motion planning and control approach is that obstacles can be readily incorporated onto the potential field, overcoming the need to search for an explicit trajectory to circumvent them (which is a formally hard problem [19]). Fig. 10 shows a run on the VDA surface where a static obstacle to the left of the vehicle's nominal path induces a potential, leading the vehicle to smoothly circumvent the obstacle.

VI. CONCLUSION

We have demonstrated that an integrated motion planning and control system based on potential fields and torque steering actuation is a feasible approach to command an autonomous vehicle. The approach is simple to implement and allows to readily incorporate the presence of obstacles in the environment to circumvent them, with no need of expensive planning or numerical optimization to find an explicit trajectory. Further, in a comparison with a SWA-based steering controller our approach achieves similar path tracking error at a significantly lower control effort.

ACKNOWLEDGMENT

The authors are sincerely grateful to Doug Rhode, Chris Attard, and Schuyler Cohen from Ford Motor Co. for helping with the experiments of this work.

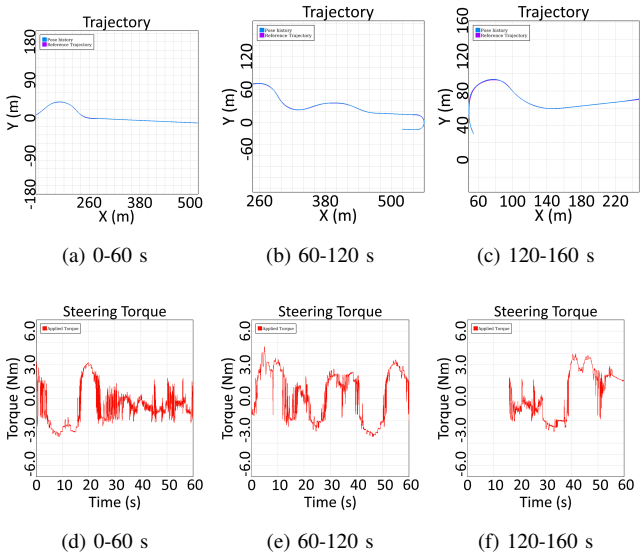

(a) 0-60 s (b) 60-120 s (c) 120-160 s

(d) 0-60 s (e) 60-120 s (f) 120-160 s

Fig. 7: Sections of the vehicle's executed trajectory (top row) and applied torque by the SWA controller (bottom row) on a trial on the SHC.

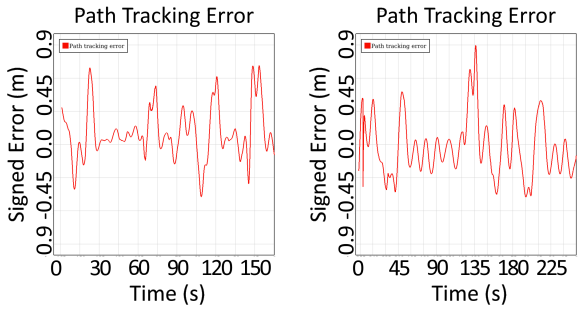

(a) Our approach (b) SWA controller

Fig. 8: Path tracking error performance of our proposed approach and a SWA-based controller on a trial on the SHC. The proposed approach, as currently tuned, has roughly the same peak-to-peak deviation as the SWA approach, but achieves lower torque effort (see Fig. 9) at the cost of slightly higher path tracking error.

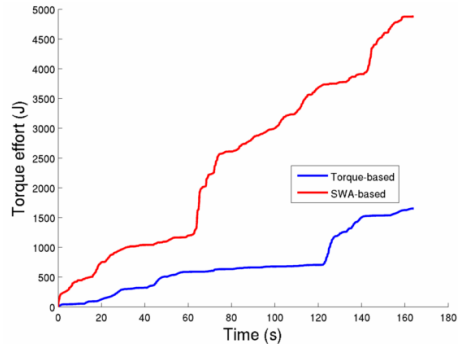

Fig. 9: Torque effort (work done by the steering actuator) exhibited by our proposed approach and a SWA-based controller on a trial on the SHC. The proposed approach requires a significantly lower torque effort.

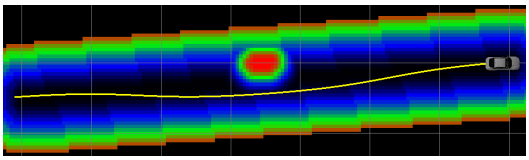

Fig. 10: Trajectory traced by our vehicle (yellow line) using a potential field with an obstacle component.

References

[1] S. Thrun *et al.*, "Stanley: The robot that won the darpa grand challenge," *J. Field Robot.*, vol. 23, no. 9, pp. 661–692, 2006.

[2] P. Falcone, F. Borrelli, J. Asgari, H. Tseng, and D. Hrovat, "Predictive active steering control for autonomous vehicle systems," *IEEE Trans. Control Syst. Technol.*, vol. 15, no. 3, pp. 566–580, May 2007.

[3] C. Urmson *et al.*, "Autonomous driving in urban environments: Boss and the urban challenge," *J. Field Robot.*, vol. 25, no. 8, pp. 425–466, 2008.

[4] DARPA, "Darpa urban challenge," http://archive.darpa.mil/grandchallenge/, 2007.

[5] J. Barraquand, B. Langlois, and J.-C. Latombe, "Numerical potential field techniques for robot path planning," *IEEE Trans. Syst., Man, Cybern.*, vol. 22, no. 2, pp. 224–241, Mar 1992.

[6] M. Likhachev and D. Ferguson, "Planning long dynamically feasible maneuvers for autonomous vehicles," *Int. J. Robot. Res.*, vol. 28, no. 8, pp. 933–945, 2009.

[7] Y. Kuwata, S. Karaman, J. Teo, E. Frazzoli, J. How, and G. Fiore, "Real-time motion planning with applications to autonomous urban driving," *IEEE Trans. Control Syst. Technol.*, vol. 17, no. 5, pp. 1105–1118, Sept 2009.

[8] J. Hardy and M. Campbell, "Contingency planning over probabilistic obstacle predictions for autonomous road vehicles," *IEEE Trans. Robot.*, vol. 29, no. 4, pp. 913–929, Aug 2013.

[9] R. Geraerts and M. H. Overmars, "Creating high-quality paths for motion planning," *Int. J. Robot. Res.*, vol. 26, no. 8, pp. 845–863, 2007.

[10] R. Wein, J. van den Berg, and D. Halperin, "Planning high-quality paths and corridors amidst obstacles," *Int. J. Robot. Res.*, vol. 27, no. 11-12, pp. 1213–1231, 2008.

[11] D. Dolgov *et al.*, "Path planning for autonomous driving in unknown environments," in *Experimental Robotics*, ser. Springer Tracts in Advanced Robotics, O. Khatib, V. Kumar, and G. Pappas, Eds. Springer Berlin Heidelberg, 2009, vol. 54, pp. 55–64.

[12] M. T. Wolf and J. Burdick, "Artificial potential functions for highway driving with collision avoidance," in *Proc. IEEE Int. Conf. Robot. and Automation*, May 2008, pp. 3731–3736.

[13] Y. Koren and J. Borenstein, "Potential field methods and their inherent limitations for mobile robot navigation," in *Proc. IEEE Int. Conf. Robot. and Automation*, Apr 1991, pp. 1398–1404.

[14] M. Nagai, H. Mouri, and P. Raksincharoensak, *The Dynamics of Vehicles on Roads and on Tracks*. Swets & Zeitlinger, 2003, ch. Vehicle lane-tracking control with steering torque input, pp. 267–278.

[15] M. Werling, L. Groll, and G. Bretthauer, "Invariant trajectory tracking with a full-size autonomous road vehicle," *IEEE Trans. Robot.*, vol. 26, no. 4, pp. 758–765, Aug 2010.

[16] D. Ferguson, T. M. Howard, and M. Likhachev, "Motion planning in urban environments," *J. Field Robot.*, vol. 25, no. 11-12, pp. 939–960, 2008.

[17] J. Hardy, M. Campbell, I. Miller, and B. Schimpf, "Sensitivity analysis of an optimization-based trajectory planner for autonomous vehicles in urban environments," in *Proc. SPIE*, vol. 7112, no. 1, 2008, p. 711211.

[18] R. C. Coulter, "Implementation of the pure pursuit path tracking algorithm," Robotics Institute, Pittsburgh, PA, Tech. Rep. CMU-RI-TR-92-01, Jan. 1992.

[19] J. Reif, "Complexity of the mover's problem and generalizations," in *20th Annual Symp. on Found. of Comp. Sci.*, Oct 1979, pp. 421–427.